Extraction of Mechanical-Reactivity Influences from Neutron Noise Spectra at the IBR-2 Reactor *

M. Dima[1**], Yu. Pepelyshev[2]

[1]*Institute for Physics and Nuclear Engineering, DFCTI, Romania*
[2]*Joint Institute for Nuclear Research, FLNP, RU-141980 Dubna, Moscow, Russia*

(Received 15 October 2012)

Neutron noise spectra in nuclear reactors are a convolution of multiple-induced reactivities. For the IBR-2 pulsed reactor (JINR-Dubna), one part is represented by the reactivities induced by the two moving reflectors, and the other part by other sources that are moderately stable. In the present study, using recordings of the mechanical noise of the two moving reflectors, their non-linear correlations into the power spectra of the reactor are extracted using statistical analysis. The remaining noise sources are moderately stable noise and can be further monitored by other automated reactor diagnoses.

PACS: 28.41.−i, 28.41.Rc, 28.41.My, 28.41.Te DOI: 10.1088/0256-307X/30/7/072801

Neutronic processes in nuclear reactors have a probabilistic character due to the quantum mechanics of scattering and the stochastics of propagation in materials. Design is mostly performed on the equations of neutron flux transport (in energy and space) and the associated effects (fission, thermal fluxes, etc). Statistical deviations from average quantities give, however, a complete image of the neutron physics in the reactor, i.e. the so-termed *neutron noise*, described largely using Markov-chain theories. The theories associated with the underlying stochasticity that produces said fluctuations are actually a century old,[1] stemming from population studies. It was thus shown that (Alphonse) de Candolle's conjecture on the extinction of family names[2] leads the case of neutron chains to non-ergodic behavior. Such theories were picked up in nuclear physics by Feynman, de Hoffmann and others to describe neutron processes in fission,[3] leading to the Feynman α-formula

$$\frac{\sigma_Z^2(t)}{\langle Z(t)\rangle} = 1 + \epsilon\Big(1 - \frac{1 - e^{-\alpha t}}{\alpha t}\Big), \qquad (1)$$

which shows the fluctuations (1) being over-Poissonian (due to correlations of neutrons in the same chain), and (2) the neutrons produced in the same group statistically disappearing (exponentially) all at the same time. The modern theoretical approach is given by the Pal-Bell equation,[4] as an applied case of the Chapman–Kolmogorov master equation to Markov-chain neutron processes. Complexity-based pattern recognition analysis is one of the modern technologies applied today.[5]

In addition to the neutron stochastic behavior is the modulation of the neutron flux by various reactivities: some due to two-phase liquid flow (bubbling), or fuel embrittlement, mechanically induced reactivities, etc. Any addition to the spectrum may be detected and classified, issuing a specific warning. In this respect, neutron noise spectrum analysis is a far reaching tool in nuclear safety.

The problem, however, is that all the effects are convoluted and that each individual pseudo-transfer function (non-linear relation through which a source noise spectrum reflects in the reactor's power noise spectrum) may be quite complicated.

In this respect, it is important to "subtract" all known influences such as to have a "pure physics" spectrum, in which any stray effect is easily spotted.

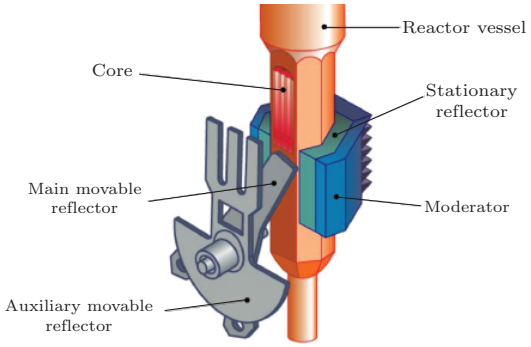

Fig. 1. Details of the IBR-2 reactor showing the active core and two movable reflectors.

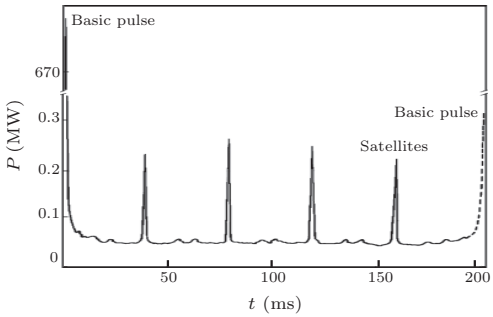

Fig. 2. The reactor pulse structure: four satellite pulses with a smaller intensity of roughly 2800 are present in between the basic pulses.

The IBR-2[6] is a 2 MW nominal power pulsed fast research reactor with PuO_2 fuel elements. The reactor coolant is liquid sodium. The pulsed mode of IBR-2 operation is enabled by a reactivity modulator consisting of two rotating parts: the main movable reflector (OPO, at 1500 rpm) and the movable reflector (DPO, at 300 rpm), as shown in Fig. 1. Each reflector creates reactivity pulses. For nominal DPO rotation speed, the reactivity of every fifth pulse is positive, i.e. the

*Supported by the Romanian National Authority for Scientific Research, CNCS-UEFISCDI, under Grant No PN-II-ID-PCE-2011-3-0323, and the JINR-Dubna order Nr.71, item 21/2012.
**Corresponding author. Email: modima@nipne.ro

reactor becomes prompt neutron-supercritical for ca. 0.400 ms (0.215 ms half-width), with a repetition frequency of 5 Hz (Fig. 2). As a result, powerful power pulses of 5 Hz repetition frequency take place in the reactor.

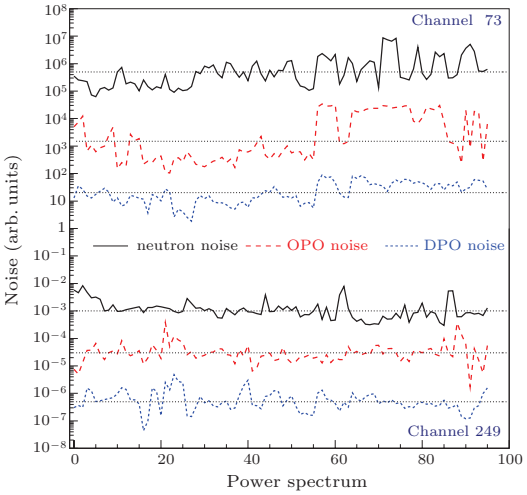

Fig. 3. Degradation of the power spectrum due to the mechanical noise of the OPO and DPO reflectors in frequency channel 73 versus channel 249. It can be observed that the power noise vibrations are correlated to a joint increase in noise levels (in the respective channels) of both the OPO and DPO reflectors. The quantities plotted are the FFT values in each frequency bin 73 and 249 (approximately 0.7 Hz and 2.5 Hz) normalized (on log-scale) to the average over the full sample of 96 spectra.

The pulsed operation mode of the reactor is established when the prompt neutron supercriticality $(\delta k - \beta)$ reaches the "equilibrium" value $\epsilon_m = \epsilon_{m0} \simeq 1 \cdot 10^{-3}$ (at 5 Hz), at which the reactor can be periodically pulsed. For supercriticality smaller than the "equlibrium" value, the amplitude (and consequently the energy) of each subsequent pulse is smaller than that of the previous one, which means that the reactor is attenuating. There are two main causes for pulse energy fluctuation in the IBR-2 reactor: the stochastic character of fission and neutron multiplication processes, and the fluctuation of external reactivity. Stochastic noise dominates power fluctuations at low neutron intensity for powers below 1 W. Pulse energy fluctuations at high power have adverse effects on the operation of the IBR-2 reactor: in the dynamics, startup and adjustment process, the performance of the experimental equipment, etc. However, the power fluctuations also have a positive aspect as a tool for reactor diagnosis. The most important characteristic of a pulsed reactor is the relative dispersion of pulse energy fluctuations, which is a convolution of stochastic fluctuations and external reactivity fluctuations. All the noise diagnostics of the reactor are based on research into this noise component.

During the reactor operation time, slow degradation (change in the shape of the spectra) of the power noise is observed, mainly due to the degradation of the mechanical vibrations of the movable reflectors,[7] see Fig. 3. It is seen that some channels remain relatively steady (channel 249, approximately 2.5 Hz), while others (channel 73, approximately 0.7 Hz) degrade over time. Other parts of the spectrum represent uncontrolled sources of the reactivity (vibrations of fuel elements, changes in the coolant density and flow rate, etc). The vibration states of the movable reflectors are represented by a set of FFT spectra of their axial oscillations (towards the core) measured during reactor operation. Reactor power noise spectra were obtained by pulse energy measurements with an ionization fission chamber. The frequency range for all spectra is 2.5 Hz (the Nyquist frequency of the 5 samples/s acquisition rate, and half the energy repetition frequency of the pulses). The total number of FFT intervals ("channels") is 256, plus a zero channel (0.00973 Hz/channel). The collection of spectra is 96 (roughly three years of reactor operation), and the vibrational spectra of the moving reflectors were measured with accelerometers.

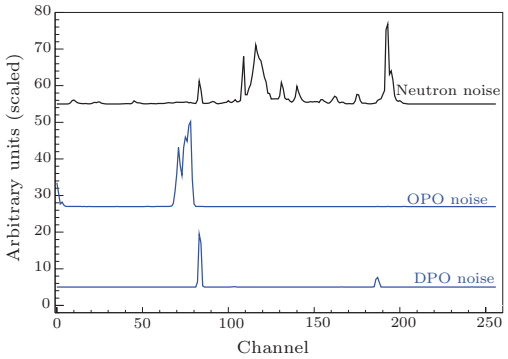

Fig. 4. Comparison of the noise standard deviations of the subtracted spectra in each frequency bin for the power noise and mechanical noise of the OPO and DPO reflectors. The vertical offsets are arbitrary and used to visualize all three spectra in the same plot.

Operative diagnostics and the prediction of noise behavior with time mean separating the reflector degradation trend in the power noise, since the reflectors "contaminate" the spectrum in a non-anticipatable manner. Thus, if the pseudo-transfer functions are known and the reflector mechanical noise is measured, then said contamination may be taken out, leaving only moderately stable noise sources in the spectrum.

The first idea in such an analysis is to verify the correlations between the power noise spectra and the mechanical vibration noise spectra of the two moving reflectors. The result is not an encouraging one, as there is very little linear correlation; see Fig. 4. The figure shows the standard deviations of the subtracted spectra computed for each frequency bin over the full sample of 96 spectra. When there is a large spread in values in the reflectors, we would expect the same in the power noise. Qualitatively this is true, however, not in the first-order (linearly). It is not surprising that since the reflectors were designed to give very sharp power pulses, then the pseudo-transfer functions should be expected to be highly nonlinear. The next option is to find analytical expressions of the pseudo-transfer functions that describe how the Fourier transform of the OPO/DPO mechanical vibrations reflect in the Fourier spectrum of the neutron noise. For this, a similar, but significantly more complex statistical

analysis has to be performed. Let the power noise spectrum be denoted by z, representing any of the 0+256 channels (available in 96 spectra):

$$\delta z = \sum_{i,j}^{N} C_{ij}\delta[f_i(x)g_j(y)] + \rho, \tag{2}$$

where x is the vibrational noise spectrum of the OPO and y of the DPO. The functions f and g are a polynomial base set of functions with which non-linearity will be modeled. The δ's represent variations in the quantities around the average. The coefficients C_{ij} minimize the error of the fit, and ρ is the residual, which should not contain any "overlap" with the terms in the sum (or else the sum is not correctly determined). By overlap it is understood that none of the terms are statistically correlated with ρ. Thus, ρ is just a random residual, hence minimal:

$$\langle\rho^2\rangle = \left\langle\left(\delta z - \sum_{i,j}^{N} C_{ij}\delta[f_i(x)g_j(y)]\right)^2\right\rangle = \min, \tag{3}$$

where the angled brackets denote the statistical average. Let $\phi_{mn}(x,y) = f_m(x)g_n(y)$, with f being a polynomial of order m and g of order n. By taking the derivative with respect to all C_{ij}, the minimization procedure yields:

$$\sum_{i,j}^{N}\langle\delta\phi_{mn}\delta\phi_{ij}\rangle C_{ij} = \langle\delta z\delta\phi_{mn}\rangle \tag{4}$$

and by inversion C_{ij} is obtained in all orders theoretically.

In practice, the inversion is a complete disaster due to the innumerous inter-correlations of the terms. For illustration purposes, consider the first-order ($i+j=1$), $\mathcal{O}_I$:

$$\begin{pmatrix} C_{01} \\ C_{10} \end{pmatrix} = \frac{1}{\Delta}\begin{pmatrix} \langle\delta^2 f\rangle & -\langle\delta f\delta g\rangle \\ -\langle\delta f\delta g\rangle & \langle\delta^2 g\rangle \end{pmatrix}\begin{pmatrix} \langle\delta z\delta g\rangle \\ \langle\delta z\delta f\rangle \end{pmatrix}, \tag{5}$$

where $\Delta = \langle\delta^2 f\rangle\langle\delta^2 g\rangle - \langle\delta f\delta g\rangle^2$ is zero for f and g is correlated. What happens in practice is that such terms are correlated to quite a degree, and hence $\delta g = \delta f + \epsilon\delta\gamma$, where γ is a function with small correlation to f and ϵ a small parameter:

$$\begin{aligned} C_{01} &= \epsilon^{-1}\frac{\langle\delta^2 f\rangle\langle\delta z\delta\gamma\rangle - \langle\delta f\delta\gamma\rangle\langle\delta z\delta f\rangle}{(1-\alpha^2)\langle\delta^2 f\rangle\langle\delta^2\gamma\rangle}, \\ C_{10} &= -C_{01} + \frac{\langle\delta^2\gamma\rangle\langle\delta z\delta f\rangle - \langle\delta f\delta\gamma\rangle\langle\delta z\delta\gamma\rangle}{(1-\alpha^2)\langle\delta^2 f\rangle\langle\delta^2\gamma\rangle}, \end{aligned} \tag{6}$$

where α is the correlation coefficient[8] between f and γ, $\alpha \simeq 0$. Both coefficients are singular for $\epsilon \to 0$. However, in terms of f and γ:

$$C_{01}\delta g + (-C_{01} + C)\delta f = C\delta f + \underbrace{(\epsilon\cdot C_{01})}_{\text{finite}}\delta\gamma, \tag{7}$$

the expression is well behaved.

This is nothing but a statement for using a procedure in which the polynomials are determined in increasing order, and the next order is always uncorrelated with all the previous polynomials. To do this, the computer code starts with the highest term of the next order. It then subtracts the polynomial part correlated to the previous polynomial in rank in the set. From what is left, the previous one is subtracted and so on till the set is exhausted. What is left will be uncorrelated to all polynomials in the set. The polynomials have a single term for $\mathcal{O}_{\text{zero}}$, two terms for $\mathcal{O}_{\text{I}}$, three for $\mathcal{O}_{\text{II}}$ and $k+1$ for $\mathcal{O}_k$. The complete expression in $\mathcal{O}_k$ has $n = (k+1)(k+2)/2$ terms, respectively, and 65 terms for $\mathcal{O}_X$ (since the $\mathcal{O}_{\text{zero}}$ is not needed).

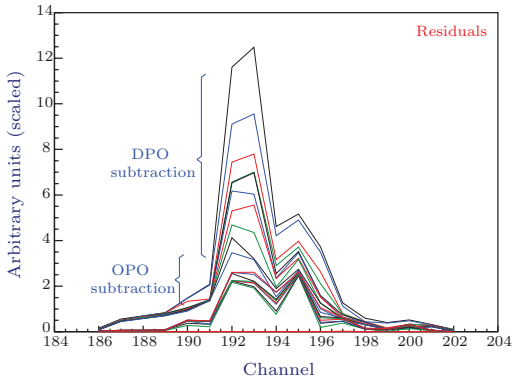

Fig. 5. The result for consecutive uni-dimensional (1D) subtraction of DPO (in increasing order, from $\mathcal{O}_{\text{I}}$ to $\mathcal{O}_{\text{IX}}$) and OPO vibrational influences (in increasing order, from OI to OIX) around channel 195 is shown. The quantities plotted are the standard deviations of the subtracted spectra in each frequency bin over the full sample of 96 spectra.

After finding the coefficients, the pseudo-transfer function can be used to take out the OPO/DPO vibrational influences from the power spectrum:

$$\langle\rho^2\rangle = \left\langle\left(\delta z - \sum_{i,j}^{N} C_{ij}\delta[f_i(x)g_j(y)]\right)^2\right\rangle, \tag{8}$$

where the average for each channel is taken over its entries in the 96 spectra of the collection. The result for consecutive uni-dimensional (1D) subtraction of DPO (in increasing order, from $\mathcal{O}_{\text{I}}$ to $\mathcal{O}_{\text{IX}}$), then OPO vibrational influences (in increasing order, from $\mathcal{O}_{\text{I}}$ to $\mathcal{O}_{\text{IX}}$) around channel 195 is shown in Fig. 5. The quantities plotted are the standard deviations of the subtracted spectra in each frequency bin over the full sample of 96 spectra. This channel seems to be correlated to the DPO and OPO vibrational noise spectra.

It can be seen that consecutive 1D-subtraction (DPO then OPO) does not flatten out the combined influence, and that true 2D correlations (OPO and DPO) are needed; see Fig. 6. The quantities plotted are the standard deviations of the subtracted spectra in each frequency bin over the full sample of 96 spectra.

The spectrum remains almost the same after subtracting polynomials up to X^{th} order (65 polynomials), less the major resonance around channel 195. However, two small peaks are uncovered at channels

118 and 123, see Fig. 7, and these will be examined to discover what they are. The quantities plotted are the standard deviations of the subtracted spectra in each frequency bin over the full sample of 96 spectra.

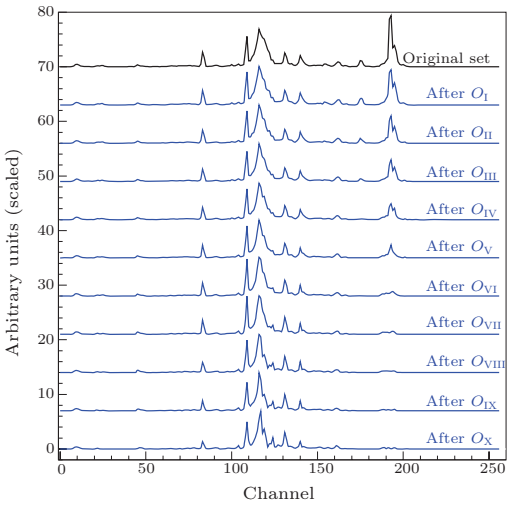

Fig. 6. The result for simultaneous (2D) subtraction of OPO and DPO vibrational influences, from $\mathcal{O}_{\rm I}$ to $\mathcal{O}_{\rm X}$. The quantities plotted are the standard deviations of the subtracted spectra in each frequency bin over the full sample of 96 spectra.

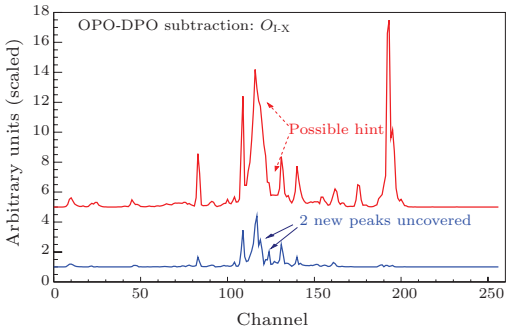

Fig. 7. Two small peaks uncovered at channels 118 and 123 after the correlated pedestal is subtracted. The quantities plotted are the standard deviations of the subtracted spectra in each frequency bin over the full sample of 96 spectra.

The spectra were scaled to have the main peak at 115 of the same amplitude. However, as correlative information is subtracted, the pedestal (the plateau underneath the peaks) does go down; see Fig. 8. The quantities plotted are the standard deviations of the subtracted spectra in each frequency bin over the full sample of 96 spectra. This region is significant in that it displays both correlated and non-correlated peaks, and correlated and non-correlated pedestals. The full spectrum cannot be visualized in its entirety, rather section by section, with this section being the most illustrative.

An example of how a pseudo-transfer function looks (for scaled entries up to a maximum of the OPO and DPO for channel 118) is given in Fig. 9. The plotted function gives the expected amplitude of neutron power noise, for a given level of the DPO and OPO vibrational amplitudes.

A natural question then arises: at what order do we stop subtracting? After all, with an infinite series in the end, all information will be subtracted regardless of it being truly correlated or not. Figure 10 gives some indication in this respect.

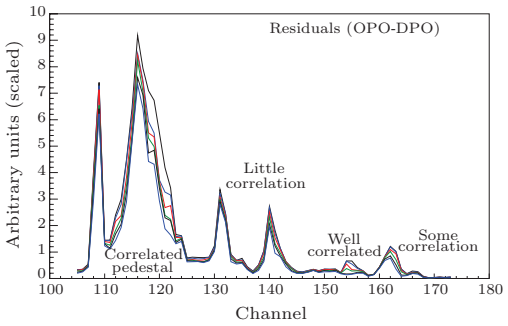

Fig. 8. Part of the spectrum showing how the procedure affects the correlated and non-correlated peaks, as well as the pedestals. The quantities plotted are the standard deviations of the subtracted spectra in each frequency bin (from $\mathcal{O}_{\rm I}$ to $\mathcal{O}_{\rm V}$) over the full sample of 96 spectra.

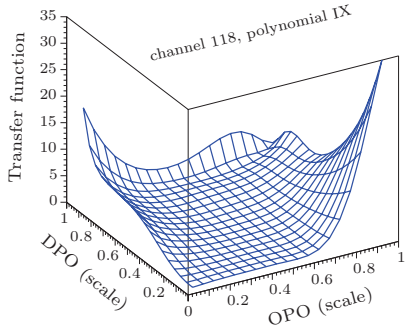

Fig. 9. Example of the pseudo-transfer function (for scaled entries up to a maximum of the OPO and DPO) for channel 118. The function gives the expected amplitude of neutron power noise for a given level of the DPO and OPO vibrational amplitudes.

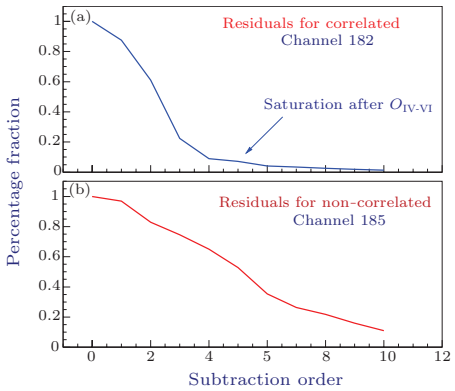

Fig. 10. The effect of subtraction for a correlated (182) and non-correlated (185) channel versus polynomial order. It can be seen that saturation occurs somewhere after $\mathcal{O}_{\rm VI}$ for the correlated channel. The quantities plotted are the standard deviations of the subtracted spectra for frequency bins 182 and 185 over the full sample of 96 spectra.

Channels with correlated information saturate somewhere after 6–7 order polynomials.

To better evidentiate the remaining data in the spectrum after subtraction, the following contrast

function is used (Fig. 11):

$$\text{contrast} = \rho\Big(\frac{\rho}{\delta z - \rho}\Big)^2, \tag{9}$$

where the quantities have been defined in Eqs. (2) and (3). The method is order-continuous and shows that 6–9 orders are sufficient to reach stability. The motivation for using such a function is to see the peaks better. It is not a physical motivation, rather one required for automated data processing (that needs to extract the position of the peaks).

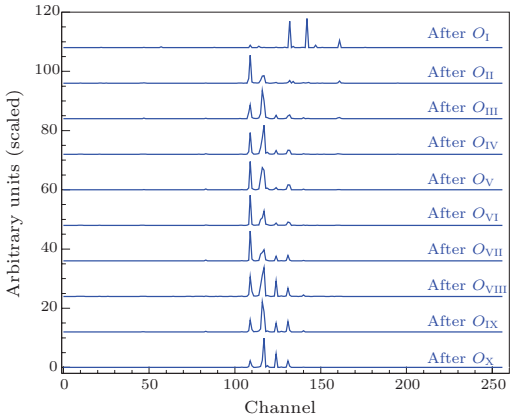

Fig. 11. Contrast function (the formula in the text) used for better evidentiating the remaining data after subtraction. It can be seen that it is order-continuous and that 9–10 orders are sufficient to reach stability.

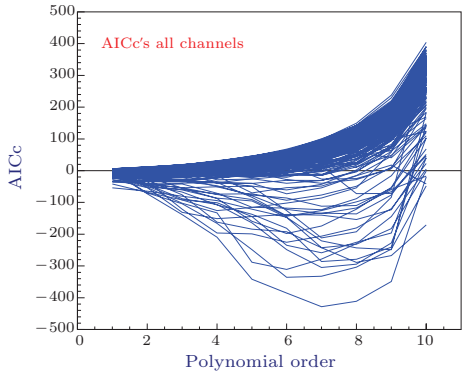

Fig. 12. The Akaike information criterion (corrected) numbers for all channels versus polynomial order. The large majority of channels show no correlation to the vibrations of the OPO and DPO reflectors. The few that do seem to reach the best parametrization for polynomial orders of V–VIII.

In principle, it could be exaggeratedly asserted that correlation does not exist in low orders, rather only in some high (unaccessible) order. How is it possible to find out? The answer is that so far, the method does not pay a cost for using innumerous parameters, an approach that at some point becomes unphysical. The Akaike information criterion[9] folds this in by adding a cost, a function of the number of parameters used, based on entropy estimates. For each frequency bin we have

$$\text{AIC}'\text{c} = \frac{2n}{1-\frac{n+1}{N}} - 2\ln L \simeq \frac{2n}{1-\frac{n+1}{N}} + N\ln(\rho/\sigma^2_{\rm eff}),$$

where N is the number of observations, n the number of parameters used, L the likelihood of the model and $\sigma^2_{\rm eff}$ the effective standard deviation (taken in this case to be that of z in each frequency bin). In the univariate normal distribution statistical model (Gaussian probability), the expression becomes a function of ρ.

Figure 12 shows the Akaike information criteria for all channels versus polynomial order. The large majority of channels show no correlation to the vibrations of the OPO and DPO reflectors. The few that do seem to reach the best parametrization for polynomial orders V–VIII. The Akaike information criteria are orientative as we do not have an exact $\sigma^2_{\rm eff}$ and may overestimate this quantity. The net effect is pulling the optimum polynomial order up to 1–2 orders higher. Since $z = z(x, y)$, we would need a statistical sample of z for each (x, y) pair, which is a luxury not available, hence the approximation of σ as $z_{\rm rms}$ in each frequency bin.

We have presented a method to correlatively remove (degrading) vibrational influences from the reactor power noise spectra, for which collateral (mechanical) noise measurements exist. The sifted spectra contain (non-degrading) stable influences, for which a contrasting function is proposed, itself stable with respect to the order in which the above subtraction is performed.

References

[1] Kendall D G 1966 *J. London Math. Soc.* **41** 385
Harris T E 1963 *The Theory of Branching Processes* (Berlin: Springer-Verlag)
[2] de Candolle A 1873 *Histoire des Sciences et des Savants*
Galton F 1873 *Educational Times Problem* 4001
Watson H W and Galton F 1875 *J. Anthropological Inst. Great Britain* **4** 138
[3] Feynman R P et al 1956 *J. Nucl. Energy* **3** 64
[4] Pal L 1958 *Nuovo Cimento Suppl.* **7** Series X, 1 25
Bell G I 1965 *Nucl. Sci. Eng.* **21** 390
Pazsit I and Pal L 2007 *Neutron Fluctuations: A Treatise on the Physics of Branching Processes* (Amsterdam: Elsevier)
Pazsit I and Enqvist A 2008 *Neutron noise in zero power systems: A primer in the physics of branching processes* (Chalmers University)
Kuang Z F and Pazsit I 2001 *Proc. R. Soc. London Ser.* A **458** 233
Pal L and Pazsit I 2006 *Phys. Scr.* **74** 62
[5] Fang C et al 2012 *Acta Phys. Sin.* **61** 170515 (in Chinese)
[6] Frank I M and Pacher P 1983 *Physica* B **120** 37
Pepelyshev Yu N and Popov A K 2006 *At. Energy* **101** 549
[7] Dzwinel W et al 2003 *Prog. Nucl. Energy* **43** 145
Pepyolyshev Yu N 2008 *Ann. Nucl. Energy* **35** 1301
Dzwinel W and Pepyolyshev Yu N 1995 *Pattern Recognition, Neutral Networks, Genetic Algorithms and High Performance Computing in Nuclear Reactor Diagnostics: Results and Perspectives, 7th Symposium on Nuclear Reactor Surveillance and Diagnostics SMORN* VII 4.5 302
Dzwinel W and Pepyolyshev Yu N 1991 *Ann. Nucl. Energy* **18** 117
[8] Myers J L and Well A D 2003 *Research Design and Statistical Analysis* (Lawrence Erlbaum) p 508
Maritz J S 1981 *Distribution-Free Statistical Methods* (Chapman & Hall) p 217
[9] Akaike H 1974 *IEEE Trans. Autom. Control* **19** 716